



C

EGYPTIAN ACADEMIC JOURNAL OF

BIOLOGICAL SCIENCES

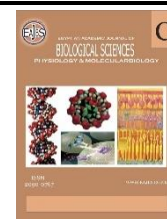
PHYSIOLOGY & MOLECULAR BIOLOGY



ISSN
2090-0767

WWW.EAJBS.EG.NET

Vol. 15 No. 1 (2023)



Structural, Thermal and Biological Efficacy with Removal Properties for Cd (II), Pb (II) of Novel poly (Acrylamide -co- Acrylonitrile)/resole semi-IPNs.

Nabaa K. Alquraishi¹, Salah S. Al-Luaibi² and Hussain J. Mohammed¹

¹Department of Chemistry, Faculty of Science, University of Kufa, Iraq.

²Department of Chemistry, Faculty of Science, University of Basra, Iraq.

*E-mail: nabaakareem281@gmail.com

ARTICLE INFO

Article History

Received:29/6/2022

Accepted:15/8/2023

Available:19/8/2023

Keywords:

Arylamide -co- acrylonitrile)/resole, semi-IPNs, morphology, adsorption, Cd (II)Pb (II).

ABSTRACT

An innovative, easy-to-use, low-cost, and selective method was developed to synthesize interpenetrating polymer networks (IPNs) as adsorbents for metal ions. The novel IPNs were characterized using various analytical techniques, including Fourier-transform infrared spectroscopy (FTIR), X-ray diffraction (XRD), scanning electron microscopy (SEM), and thermal analysis. The IPNs were synthesized using Polyacrylonitrile, polyacrylamide, and phenol-formaldehyde. The adsorption data demonstrated that the newly synthesized IPNs exhibited superior adsorption performance for metal ions. Furthermore, a comprehensive investigation was conducted to estimate the adsorption capacity of the IPNs for metal ions, focusing on Cd (II) and Pb (II). The study also examined the effects of pH and equilibrium conditions on the adsorption process, while determining the maximum reaction capacity of the metal ions. The results revealed that the (AM-co-AN)/resole semi-IPNs displayed an enhanced ability to remove Cd (II) and Pb(II) from aqueous solutions using a batch system. This study also tested an effect (AM-co-AN)/resole semi-IPNs On biological activity.

INTRODUCTION

Recently, there has been significant interest in enhancing polymer blends by incorporating a second reactive polymer to create interpenetrating polymer network systems (IPNs). IPNs are composed of two or more chemically distinct networks with interlocking at the molecular level (Sangemano.M *et al.*, 2012, Chen.S *et al.*,2011, Chen.S *et al.*,2010, Crivello. J.V,2007). Various monomer compositions have been utilized for IPN production, involving the superposition of two or more polymers with fractional interlocking at the molecular level (Moussa. K and Decher. C, 1993, Sangermano.M *et al.*,2014, decker. C *et al.*, 2001, Rajaraman.C *et al.*,1999, Jain. Y *et al.*,2013, Carioscia A.J *et al.*,2007, Dragan.S.E *et al.*,2014,lee .Y *et al.*,2008,Xiao.P *et al.*,2014,).

In this study, an IPN material was developed to effectively remove ions at lower concentrations, aiming to assess the potential of IPNs in addressing vital ion-related challenges in the future.

The term "IPN" was first introduced by John Millar in 1960 (Millar. J.R.,1960). An IPN refers to a collection of polymeric systems where there are no covalent bonds between the different polymeric networks, but they are partially interlocked on a molecular level.

Sequential IPNs can be created by dissolving the monomer of the second polymer in the first polymer network and subsequently cross-linking the second polymer to form a network. Alternatively, simultaneous IPNs can be formed by blending two monomers and cross-linking them simultaneously to generate a network. Another approach involves a two-step process: initially blending two thermodynamically miscible polymers, followed by cross-linking to form a network (Inamdar. A,1999). IPNs have garnered attention due to their superior properties compared to individual polymers or polymer blends. The wide glass transition temperature range exhibited by IPNs is advantageous for energy absorption and vibration damping, making them valuable in applications such as dental composites, damping composites, artificial teeth, tires, medical devices, and drug delivery systems. By controlling factors such as diffusivity, dissolution/erosion rate, pH, and temperature sensitivity, IPNs enable the controlled release of drugs or biologically active materials (Rudin. A ,1999, Sperling.L.H,2001).

IPNs have found application in dentistry as synthetic teeth and cavity fillers, offering benefits such as reduced shrinkage, improved bonding, and decreased temperature sensitivity. Despite their extensive commercial use, studying IPNs is challenging due to their complex nature, involving multiple chemistries, processing conditions, kinetics, thermodynamics, and instabilities. This thesis IPNs have found application in dentistry as synthetic teeth and cavity fillers, offering benefits such as reduced shrinkage, improved bonding, and decreased temperature sensitivity. Despite their extensive commercial use, studying IPNs is challenging due to their complex nature, involving multiple chemistries, processing conditions, kinetics, thermodynamics, and instabilities. This thesis aims to investigate the relationships between the structure, properties, and processing of a model IPN system (Yang. J,1996). Minimum

inhibitory concentration (MIC) is the lowest concentration of a chemical, usually a drug, which prevents visible *in vitro* growth of bacteria or fungi. MIC testing is performed in both diagnostic (Pfaller. M.A,2010) and drug discovery laboratories.

MATERIALS AND METHODS

General Procedures:

Commercially purchased solvents and chemicals from Sigma-Aldrich and Fluka, known for their highest analytical grade, were used in this study. Infrared spectra were recorded using the Bruker Alpha FT-IR spectrometer, located at the Faculty of Science, University of Kufa. X-ray diffraction (XRD) analysis was performed using the Rigaku instrument from Japan, while energy-dispersive X-ray spectroscopy (EDX) was conducted with the BRUKER X FLASH61 10 instruments at the Department of Chemistry, Faculty of Sciences, University of Tehran, Iran. The Shimadzu AA-6300 Flame Atomic Absorption Spectrophotometer was utilized for analysis in the Faculty of Pharmacy, University of Kufa. Furthermore, scanning electron microscopy (SEM) examination of S50 was conducted using the Materials Science/EFI facility at the Faculty of Science, University of Kufa.

The Synthesis of A Polymer, Acrylamide-co-Acrylonitrile:

To prepare poly(acrylamide-co-acrylonitrile), a three-neck round-bottom flask was filled with 0.0192 moles of acrylamide and 0.1728 moles of acrylonitrile. The poly(acrylamide-co-acrylonitrile) was prepared by dissolving it in 100 ml of distilled water. Along with three drops of soap solution, an emulsion of 0.01g of ferrous chloride initiator and 0.01g of potassium persulfate initiator was added to the solution. The reaction mixture was refluxed at 65°C for three hours. Afterward, the copolymers were washed several times and dried for three hours at 50°C, resulting in a light orange solid with a yield of 2.5 g of acrylamide-co-acrylonitrile.

Resole (phenol formaldehyde resin)

Synthesis:

To synthesize phenol formaldehyde resin (Resole), 0.2125 moles of phenol were dissolved in 100 ml of a 37% formaldehyde solution. The mixture was prepared in a three-neck round-bottom flask. Next, 10% sodium hydroxide was added gradually to the mixture until the pH reached 11. The resulting solution was then heated at 70°C while continuously stirring. After cooling, 5% phosphoric acid was employed to neutralize the solution. To separate the resulting mixture, tetrahydrofuran (THF) was used as a separating agent in a separating funnel. The separated solution was subsequently evaporated, and the resin was dried at 50°C for 3 hours, resulting in the formation of a dark orange phenol formaldehyde resin. The yield of the resin was 4.5 g.

Synthesis of Interpenetrating Polymer Networks Semi-IPNs:

Equal parts of phenol formaldehyde resin and copolymer (AM-co-AN) in a 1:1 ratio were thoroughly mixed and subsequently placed in an oven set at 80°C for 3 hrs. During this process, the mixture hardened effectively and underwent grinding, resulting in the formation of Interpenetrating Polymer Networks (IPNs).

Adsorption Experiments:

The uptake of metal ions was quantified by placing 0.1 g of (AM-CO-AN)/resole IPNS in a conical flask containing a solution of Cd²⁺ and Pb²⁺ metal ions at a concentration of 100 mg/L and pH 4.0. The mixture was shaken at 25°C and 180 revolutions per minute. To determine the remaining concentration of metal ions, samples were collected at intervals of 0.25, 0.5, 1, 2, and 3 hours.

To examine the effect of initial metal ion concentrations on the adsorption of Cd²⁺ and Pb²⁺ ions using (AM-co-AN)/resole semi-IPNs, 0.1 g of dried (AM-co-AN)/resole semi-IPNs was introduced into separate flasks containing 10 mL of metal ion

solutions with various concentrations (100 mg/L) and pH 4.0. The flasks were shaken for 2 hours at 180 rpm and 25°C to reach equilibrium. The concentration of residual metal ions in the solutions was determined after filtering the solids.

In addition, to study the influence of pH, 0.1 g of dry (AM-co-AN)/resole semi-IPNs was shaken with 10 mL of metal ion solutions (Cd²⁺ and Pb²⁺ at a concentration of 100 mg/L) at controlled pH values of 2, 6, and 8. The shaking process was carried out for 2 hours at 180 rpm and 25°C. The absorption efficiency of (AM-co-AN)/resole semi-IPNs was calculated using Equation (1):

$$\% \text{adsorption} = (C_i - C_f) / C_i * 100 \dots\dots(1)$$

Where: C_i (mg/L) represents the initial concentration of the metal ion before adsorption. C_f (mg/L) represents the final concentration of the metal ion in the solution after adsorption.

The spectrophotometer used for absorption measurements was the Shimadzu Spectra Instrument Model AA-6300.

Biological Efficacy:

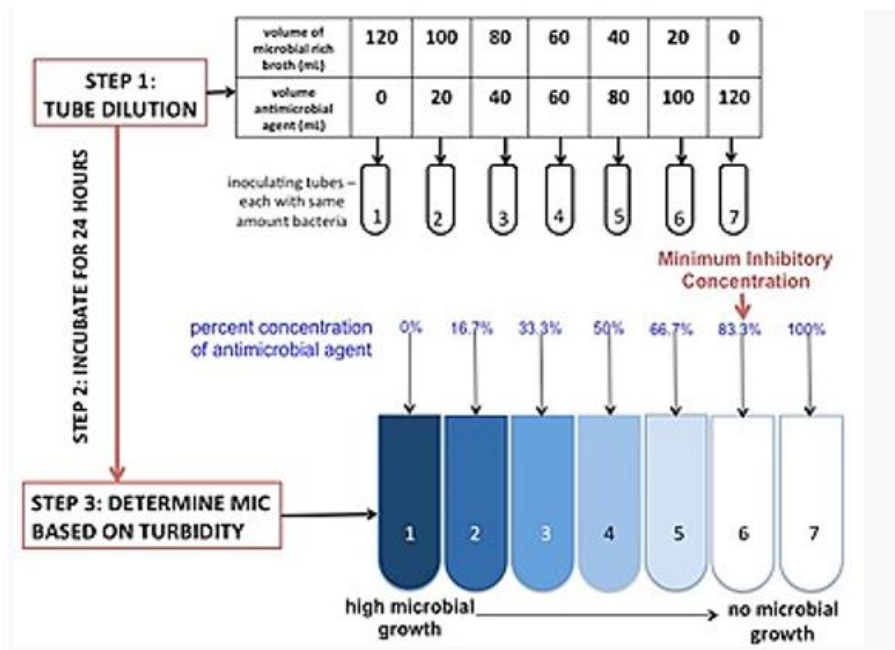
Testing the Ability of Interpenetrating Polymer Networks Semi-IPNs to Inhibit the Growth of Microbes (bacteria):

First, we choose the type of test for this process, which is:

Minimum Inhibitory Concentration (MIC): The MIC is determined by preparing a dilution series of the chemical, adding agar or broth, then inoculating with bacteria or fungi, and incubating at a suitable temperature. The value obtained is largely dependent on the susceptibility of the microorganism and the antimicrobial potency of the chemical, but other variables can affect results too. The MIC is often expressed in micrograms per milliliter (µg/mL) or milligrams per liter (mg/L).

Broth Dilution Assay:

The MIC is determined by examining tubes containing the microbe and a dilution series of antimicrobial agents for turbidity.



Schema 1: Broth Dilution Assay

There are three main reagents necessary to run this assay: the media, an antimicrobial agent, and the microbe being tested. The most commonly used media is cation-adjusted Mueller Hinton Broth, due to its ability to support the growth of most pathogens and its lack of inhibitors towards common antibiotics. Depending on the pathogen and antibiotics being tested, the media can be changed and/or adjusted. The antimicrobial concentration is adjusted to the correct concentration by mixing stock antimicrobial with media. The adjusted antimicrobial is serially diluted into multiple tubes (or wells) to obtain a gradient. The dilution rate can be adjusted depending on the breakpoint and the practitioner's needs. The microbe, or the inoculating agent, must come from the same colony-forming unit and must be at the correct concentration. This may be adjusted by incubation time and dilution. For verification, the positive control is plated in a hundredfold dilution to count colony-forming units. The microbes inoculate the tubes (or plate) and are incubated for 16–20 hours. The MIC is generally determined by turbidity. So, we will use in this test:

- 1- The media Mueller Hinton Broth
- 2- The antimicrobial agent is the poly (Acrylamide -co Acrylonitrile)/resole-semi-

IPNs.

3- The microbe used *Streptococcus pyogenes*. Here, for the purpose of dilution, DMSO (Dimethyl sulfoxide) will be used because the IPNs do not dissolve in water.

RESULTS AND DISCUSSION

The first stage of this study centered on the synthesizing of (AM-co-AN)/resole semi-IPNs. This was achieved by mixing acrylamide co-acrylonitrile with phenol-formaldehyde resin in a 1:1 ratio and then curing at 80 c for 3 hrs., resulting in the formation of (AM-co-AN)/resole semi-IPNs. (Acrylic amide + Acrylonitrile) + (Phenol formaldehyde) → (AM-co-AN)/resole semi-IPNs

FTIR Spectroscopy:

The FTIR spectra of poly (AM-co-CN) shown in Figure (1), exhibit absorption bands corresponding to stretching vibrations. The stretching vibration band (NH) appears at 3355.97 cm⁻¹, while the (CH) stretching vibration is observed at 2933.44 cm⁻¹. Furthermore, the stretching vibration of the (CN) group becomes evident at 2243 cm⁻¹. The range from 1733.36 to 1679.81 cm⁻¹ displays detectable stretching vibrations associated with the (C=O) group.

In the IR spectra of the resin, the (O-H) group is identified at 3556.99 cm⁻¹. Additionally,

the poly (AM-co-CN)/resole semi-IPNs FT-IR spectra exhibit an amine band at 3338.49 cm⁻¹. Further analysis reveals peaks at 2976.93 cm⁻¹, indicating the presence of

aliphatic (CH) groups, 2243.59 cm⁻¹, signifying the (CN) band, and 1679.50 cm⁻¹, indicating the amide (C=O) group.

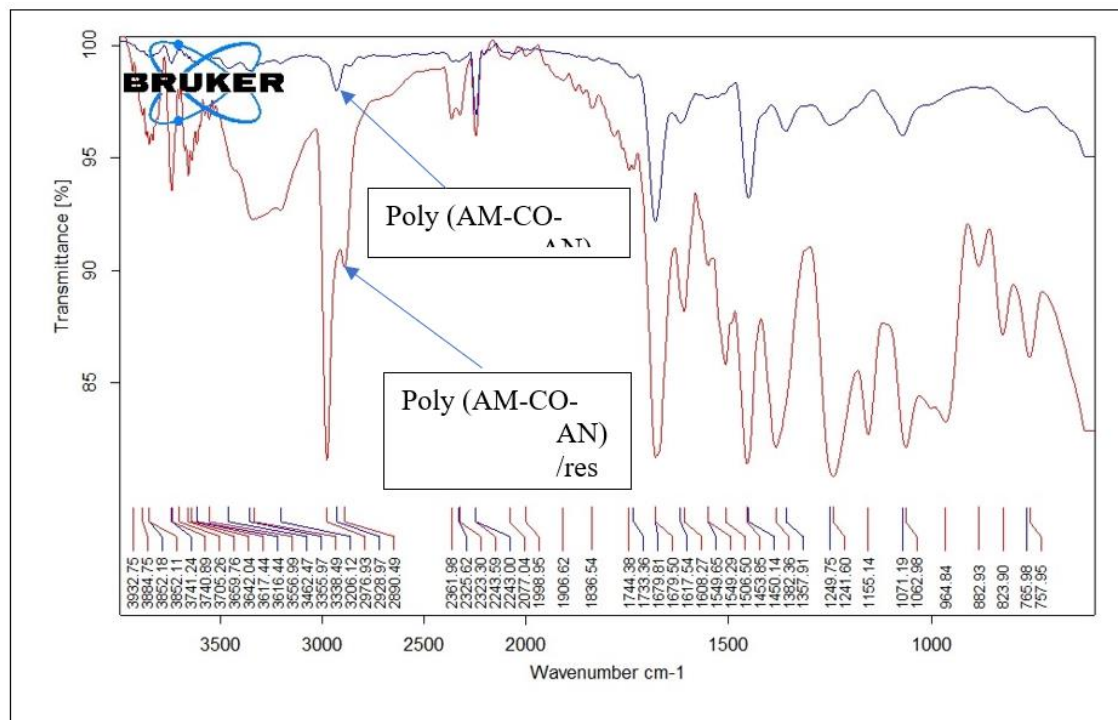


Fig 1. IR spectra for polymer (AM-CO-AN), (AM-CO-AN)/resole semi-IPNs

Thermo Gravimetric (TGA) AND (DSC):

TGA and DSC thermograms shown in Figure (2), illustrate the decomposition process of water at a temperature of 75.0°C. The first decomposition occurs below 230°C, and the weight loss observed can be attributed to nitrile cyclization (Anirudhan S.T *et al.*, 2009). The second decomposition, taking place from 265°C to 450°C, is assigned to the chain dissociation of poly (AM-co-AN). The DSC profile of poly (AM-co-AN) indicates a close relationship between cyclization and the structure of poly (AM-co-AN). The DSC curves of poly (AM-co-AN) clearly exhibit separate endothermic and exothermic peaks. A broad endothermic peak centered around 75°C is attributed to the loss of water associated with poly (AM-co-AN). The second exothermic peak, with its maximum at temperatures ranging from 265°C to 550°C, corresponds to the cyclization mechanism. It is worth noting that samples obtained at higher polymerization temperatures tend to exhibit easier cyclization. In Figure (3), the TGA events of poly (AM-co-AN)/resole semi-IPNs are presented. A decomposition process is observed between 125°C and 225°C, as well as at 475°C. The weight loss at 225°C and 475°C is attributed to the deterioration of the main structure of poly (AM-co-AN)/resole semi-IPNs. Furthermore, the weight loss occurring between 475°C and 510°C is due to the deterioration of the chain structure of poly (AM-co-AN) (A.K. Gupta. A.K *et al.*, 1996). The DSC curves of poly (AM-co-AN)/resole semi-IPNs exhibit a broad endothermic peak at approximately 125°C, which is assigned to the absorption of moisture and evaporation of residual traces. The exothermic peak, observed within the temperature range of 325°C to 525°C, corresponds to the decomposition of poly (AM-co-AN)/resole IPNs.

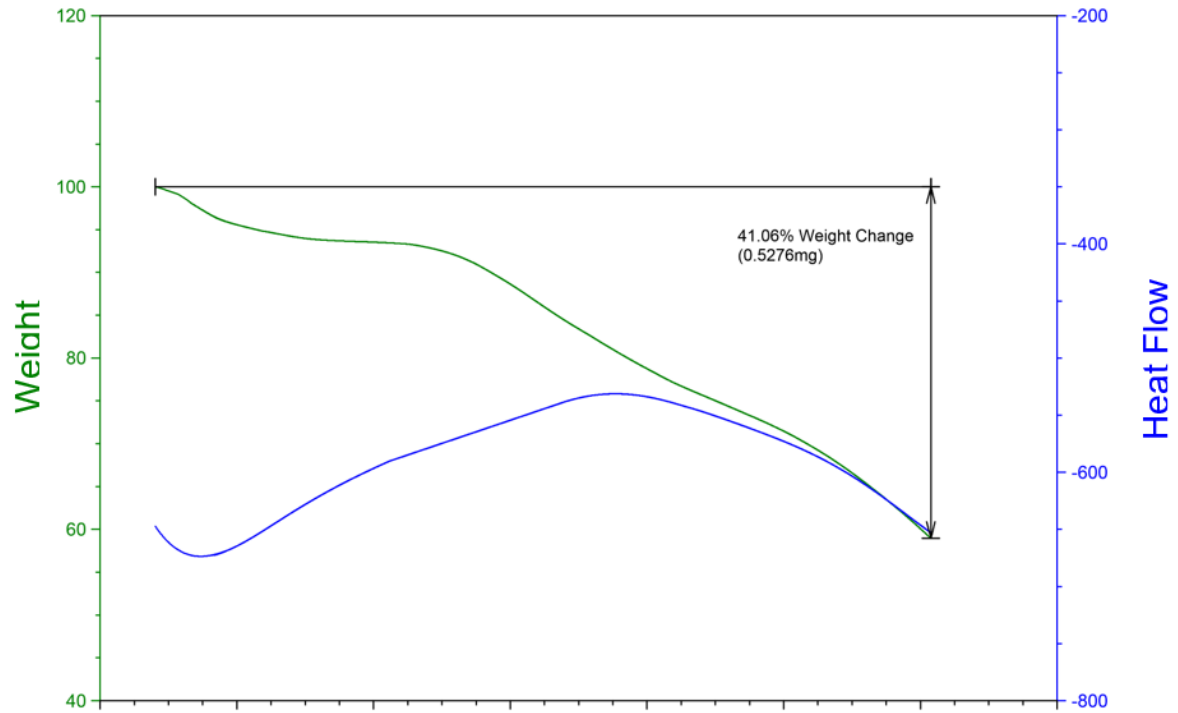


Fig 2. Thermogravimetric and differential Scanning Calorimetry profiles for poly (AM-co-AN).

Comment: 25-600@10-Ar

Instrument: SDT Q600 V20.9 Build 20

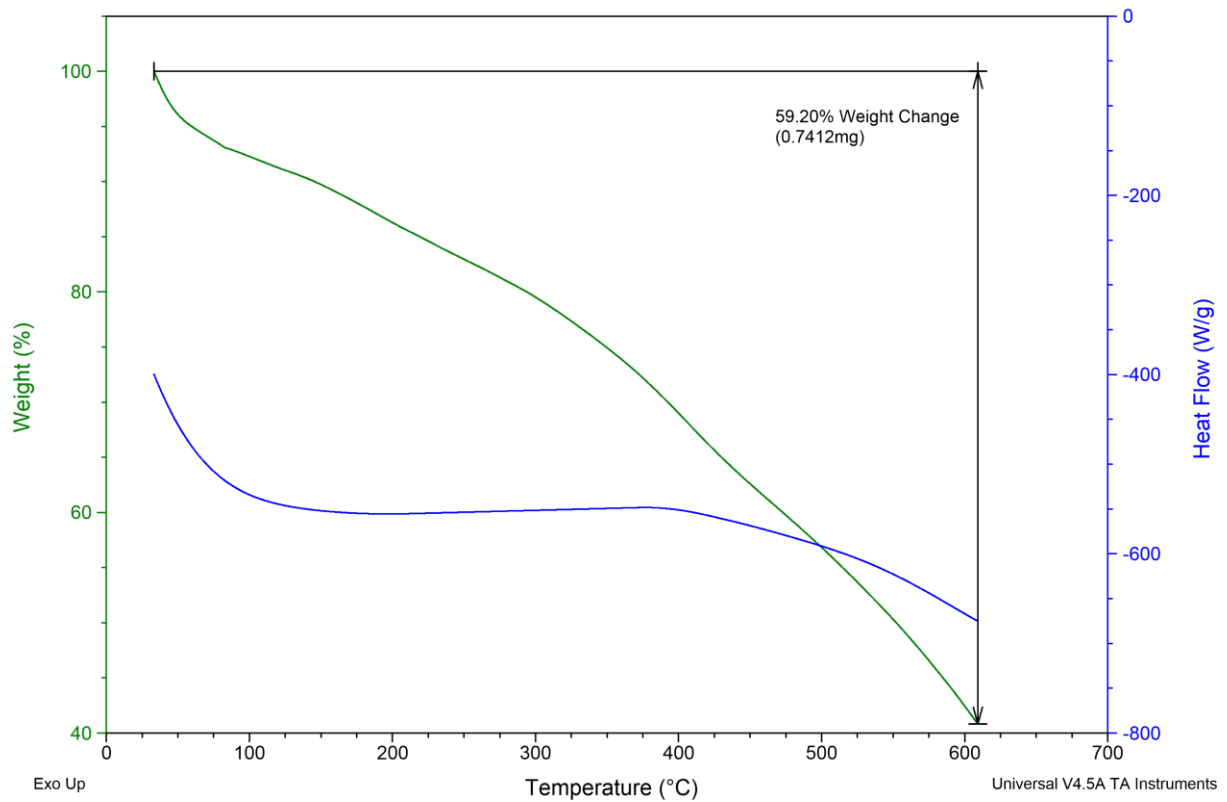


Fig 3. Thermogravimetric and differential Scanning Calorimetry profiles for poly (AM-co-AN)/resole semi-IPNs.

X-ray Diffraction:

Figure 4 shows the X-ray diffraction pattern of poly (AM-co-AN), revealing the presence of peaks at 2θ values of 17.5° and 24.2° . The first peak corresponds to the crystalline regions of the poly (AM-co-AN), while the broader second peak indicates the presence of amorphous regions (Mokhtar. S.M. *et al.*, 2014). The copolymer exhibits a

semi-crystalline structure with a low crystallinity index. Upon introducing IPNs of poly (AM-co-AN), the diffraction pattern changes, specifically a decrease in the intensity of the halo between 19.5° and $24^\circ 2\theta$. This observation suggests a reduction in the amorphous fraction of the IPNs of poly (AM-co-AN) (Fig. 5).

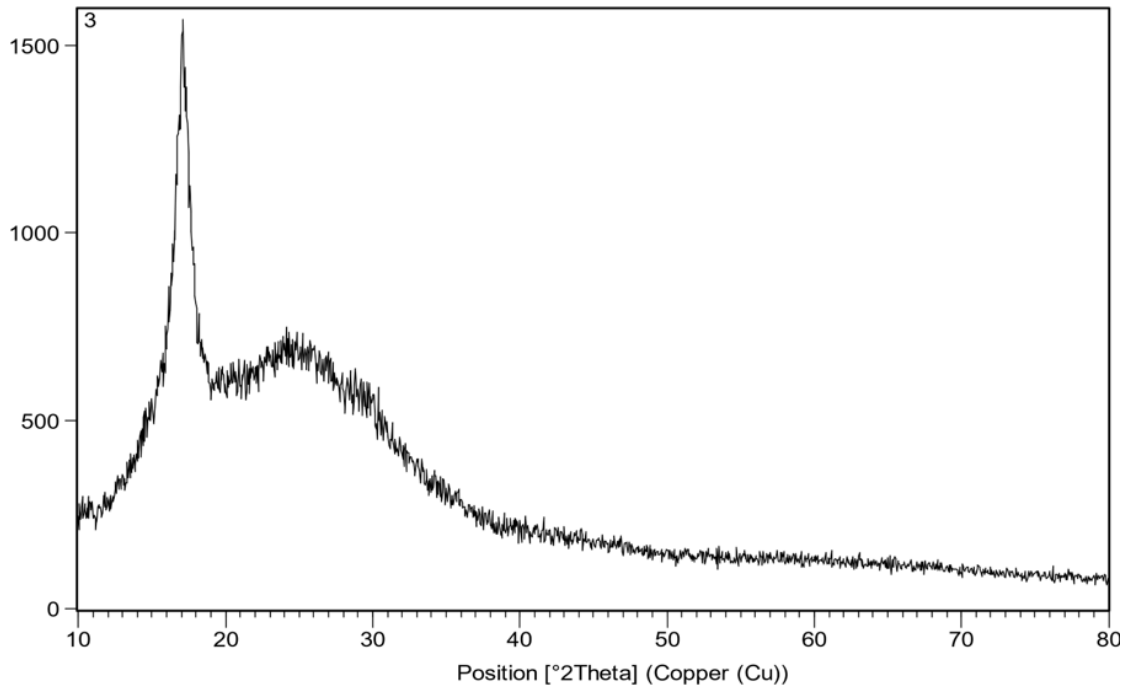


Fig 4. XRD of poly (AM-co-AN).

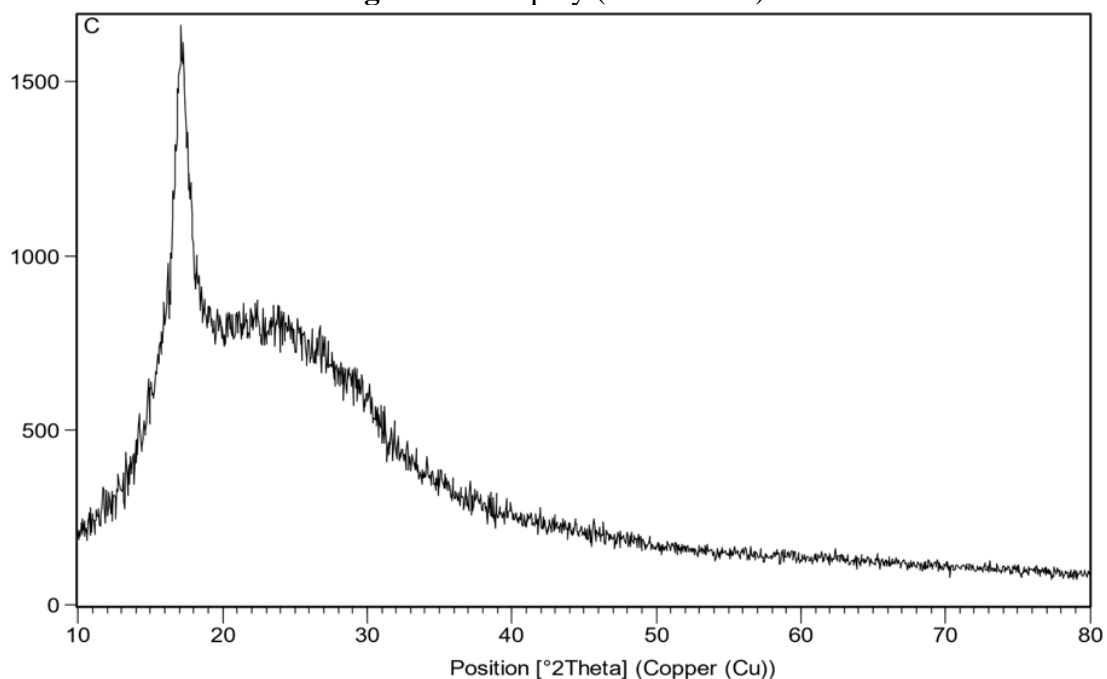


Fig 5. XRD of poly (AM-co-AN)/resole semi-IPNs

FESEM:

The surface morphology of the acryl amide/acrylonitrile copolymer (AM-co-AN), and the (AM-co-AN)/resole semi-IPNs were noticed using field emission scanning electron microscopy (SEM). It can be seen in Figure (6), that the images of (AM-co-AN) samples clearly offered irregularly shaped granular structures. The microbeads appear spherical, which is favorable for adsorption the surface morphology of (AM-co-AN) is

found to be smooth, whereas, after conversion of (AM-co-AN) to (AM-co-AN)/resole semi-IPNs, the surface morphology becomes roughner as well as the introduction resole into (AM-co-AN) increase the roughness of the Surface. Figure (7) offers that the particle size of poly (AM-co-AN)/resole semi-IPNs is ~ 150.99 nm, which is larger than that of poly (AM-co-AN) ~ 114.29 nm. (Ramya. R *et al.*,2011).

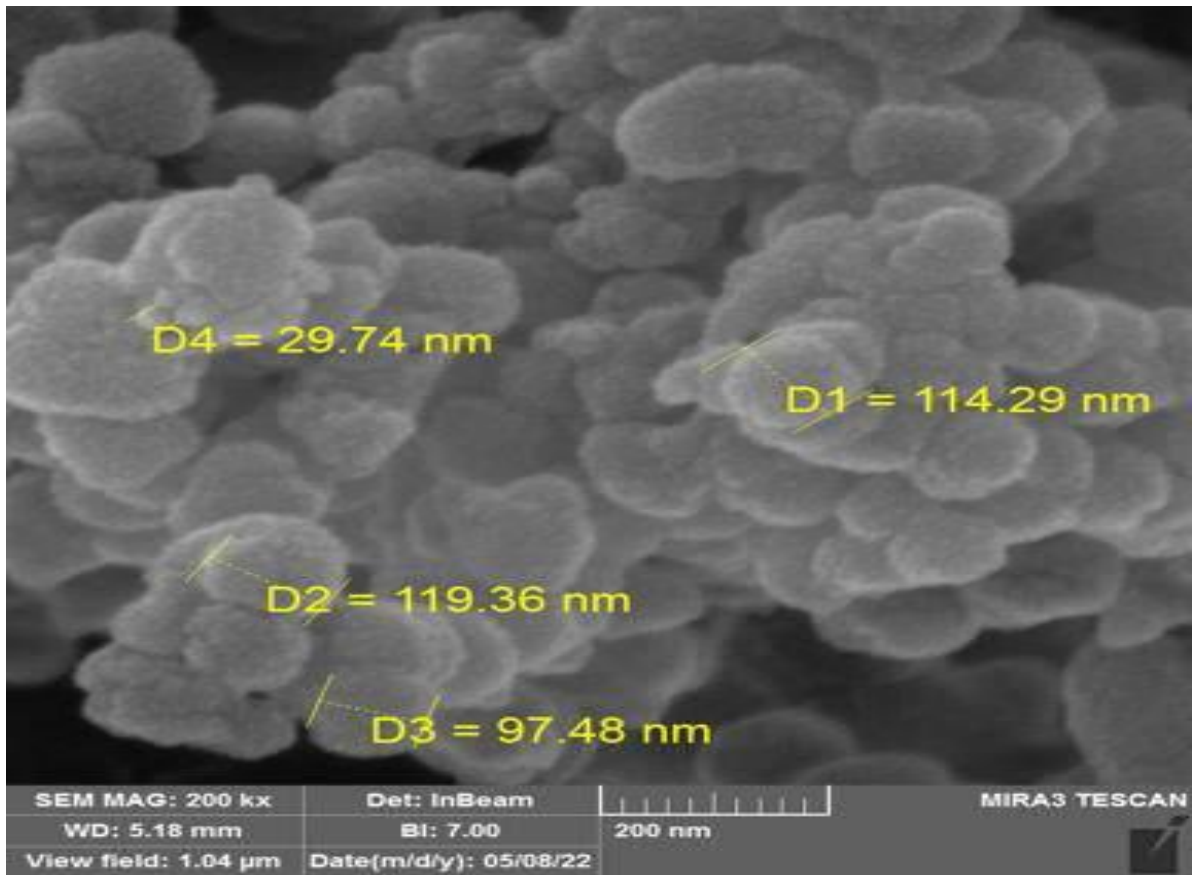


Fig 6. SEM of poly (AM-co-AN)

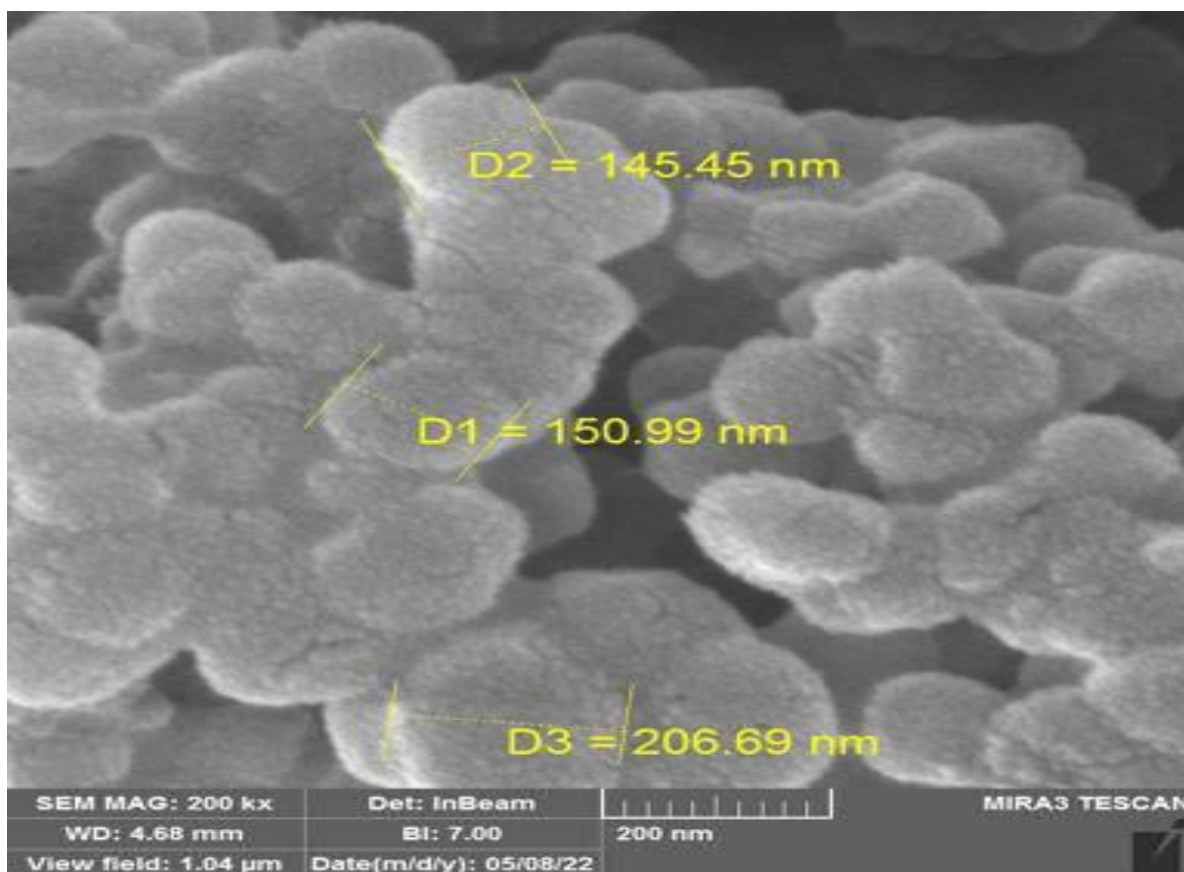


Fig 7. SEM of poly (AM-co-AN)/resole semi- IPNs

Removal of Metals Ions (Adsorption):

Adsorption percentages of cadmium and lead ions by (AM-co-AN)/resole semi-IPNs were calculated. Cation (Cd^{2+}), (Pb^{2+}) at 100 mg/L was used to precisely suspend the IPNs (AM-co-AN) and resolve in a volume of 10 ml. Adsorption of Cd^{2+} and Pb^{2+} ions from aqueous solutions was investigated as a function of pH, concentration of (AM-co-AN)/resole semi-IPNs and agitation time.

Study of Adsorption Isotherms:

20 ml of (Cd^{2+}), and (Pb^{2+}) solutions with concentrations of 5, 10, 20, 30, and 40 ppm were generated by suitably diluting the stock solution. The optimal settings for pH, adsorbent dose, adsorbent particle size, agitation speed, temperature, and contact time were chosen based on the adsorbent sample used to evaluate the adsorption isotherm. Finally, the suspensions were filtered, and the

filtrates were tested for leftover (Cd^{2+}), (Pb^{2+}) concentrations with a flame atomic absorption spectrophotometer. The Langmuir isotherm was drawn using the usual straight-line equation (2):

$$1/q = 1/b q_m c_e + 1/q_m \dots\dots (2)$$

Where 'q' (mg g^{-1}) is the quantity of metal ions adsorbed, 'Ce' (ppm) is the metal concentration at equilibrium, and q_m (mg g^{-1}) and b (L g^{-1}) are Langmuir isotherm parameters computed from the slope and intercept values of a linear plot of $1/q$ vs $1/C_e$. The Freundlich isotherm was drawn using the usual straight-line equation (3). The intercept determines the value of KF, while the slope of the linear plot of $\log q$ versus $\log C_e$ determines the value of $1/n$. KF and $1/n$ are Freundlich isotherm parameters.

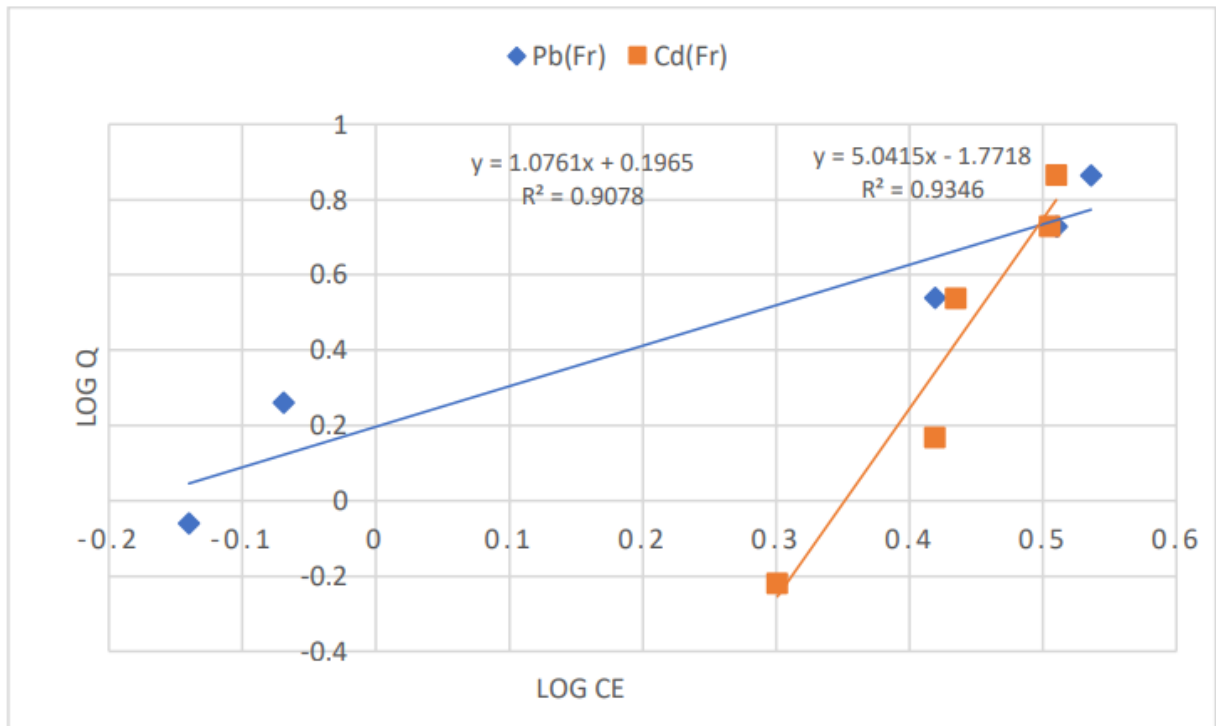
$$\log q = \log KF + 1/n \log 1/C_e \dots\dots(3).$$

Table 1. Parameters of Freundlich and Langmuir constants for Adsorption

Freundlich Isotherm Parameters	Cd ⁺²
$1/n^1$	5.0415
k_F	1.7718
R^{SF}	0.9346
Langmuir Isotherm Parameters	
Q_m (mg g ⁻¹)	8.0048
b (L g ⁻¹)	2.3963
$R^2 L$	0.9531

Table 2. Parameters of Freundlich and Langmuir constants for Adsorption

Freundlich Isotherm Parameters	Pb ⁺²
$1/n^1$	1.0761
k_F	0.1965
R^{SF}	0.9078
Langmuir Isotherm Parameters	
Q_m (mg g ⁻¹)	0.728
b (L g ⁻¹)	0.0539
$R^2 L$	0.8512

**Fig.8.** Freundlich adsorption isotherm for Pb (II), Cd (II) metals adsorption by poly (AM-CO-AN)/resole IPN's) at pH=4, shaking rate 180 rpm, amount of adsorbent 0.1g

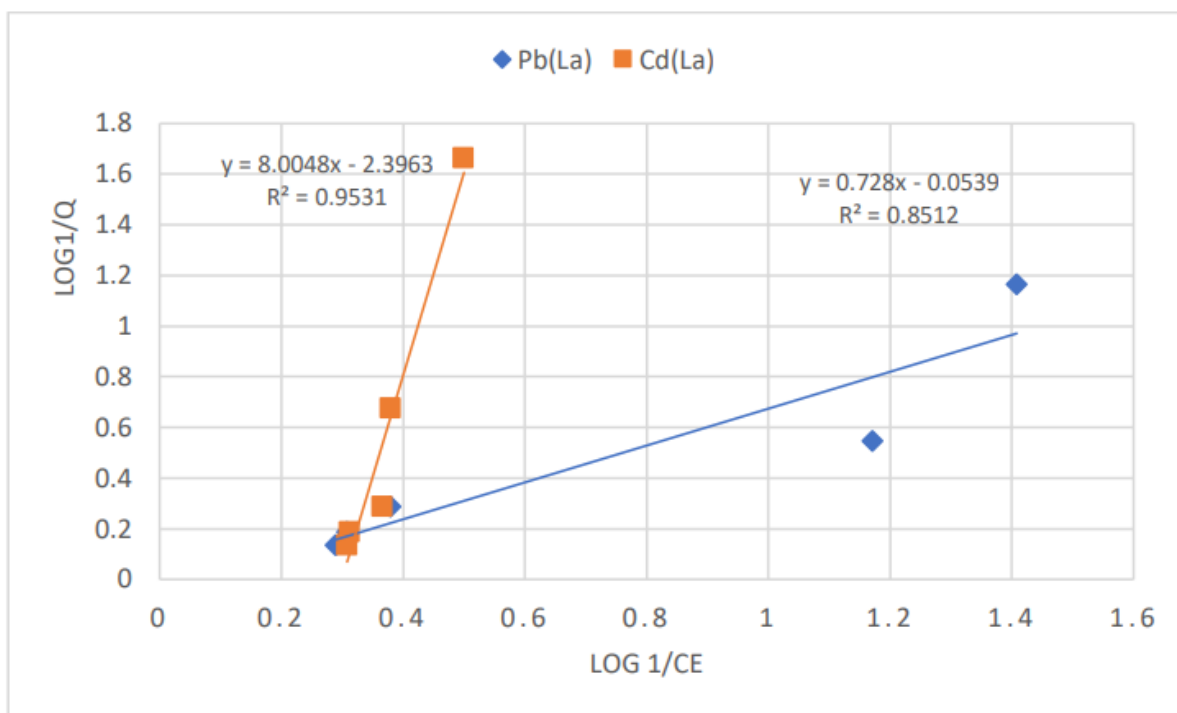


Fig. 9. Langmuir adsorption isotherm for Pb (II), Cd (II) metals adsorption by poly (AM-co-AN)/resole semi- IPN's) at pH=4, shaking rate 180 rmp, amount of adsorbent 0.1g

Adsorption Isotherms:

In this study, we varied the starting concentrations of metal ions from 5 to 40 ppm while maintaining the same adsorption dosage (0.1 g) at the optimal pH of 4. Figures 8, and 9 lists the values for the parameters of the Langmuir and Freundlich isotherms, respectively. Correlation coefficient (R^2) values for the Langmuir isotherm are higher than for the Freundlich isotherm, suggesting that the Langmuir model is a superior fit for the (Cd+2) data. Adsorption of metal ion (Cd+2) from solutions on the surface (AM-co-AN) / resole semi- IPNs created in this work can be explained using the Langmuir isotherm when the monolayer mode is employed rather than the multilayer mode. The essential premise of the Langmuir hypothesis is that sorption can occur at well-defined, homogeneous sites on the adsorption. There can be no more adsorption at a site after it has been occupied by an absorption. While we look on According to linear regression analysis, the Freundlich isotherm better fits the data than the Langmuir isotherm because the Freundlich model has a higher correlation coefficient (R^2). This

finding lends credence to the idea that, when applied in the multilayer mode rather than the monolayer mode, the Freundlich isotherm accurately describes the adsorption of metal ion (Pb+2) from solutions onto the surface of the poly (AM-co-AN) or resole semi-IPNs created in this study. Adsorption of the studied ions and IPNs is best described by the Freundlich isotherm rather than the Langmuir equation (Sangeetha. V,2013), due to the linear Application of the former.

Effect of PH:

They looked into how pH levels affected the depletion of metal ions. The elimination of metal ions, such as Cd+2 and Pb+2, depends on the abundance of oxygen atoms in acrylamide, which are attracted to the higher concentrations of H+ ions present as the solution becomes more acidic. Extra H+ ions would reduce the adsorption rate because they would compete with the Cd²⁺Pb⁺² ions.

Therefore, it is crucial to ensure that the solution pH is correct. The effect of H+ ion concentration on metal removal was studied in the pH range of 2-8. The influence of pH on the elimination of Cd²⁺ and Pb⁺²ions

by AM-co-AN/resole semi-IPNs is shown in Figure 10. The optimum pH range for cations adsorption of metals was between 4 and 6. In such an acidic environment, the ions totally dissolve and their binding to IPNs becomes

stable; also, cadmium and lead hydroxide ions begin to precipitate after an acidity of 6. At a pH of 4, metals were absorbed at the greatest rate. Therefore, the optimal pH range for the remaining experiments was determined to be.

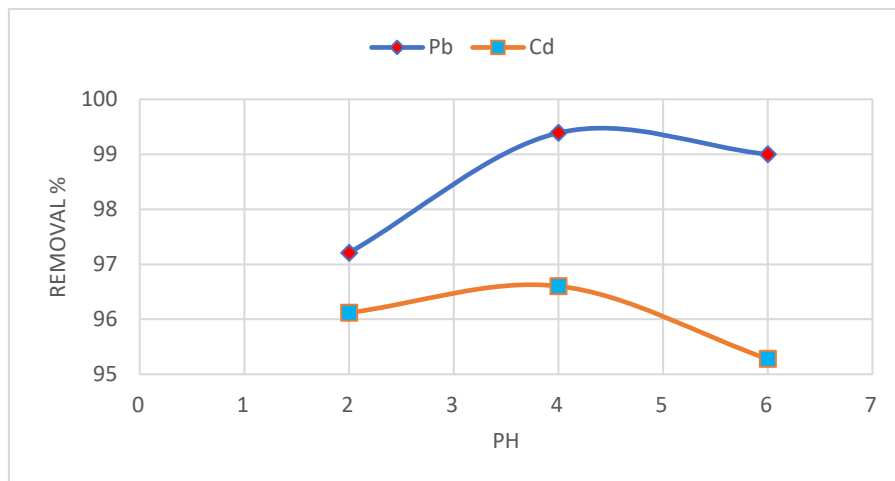


Fig.10. Effect of pH on adsorption of Cadmium ion, lead ion on (AM-co-AN)/resole semi-IPNs.

Effect of Time on Adsorption:

Adsorption equilibrium time can be estimated from contact time, making contact time a crucial metric. In order to determine the impact of contact time on poly (AM-CO-

AN) /resole semi-IPNs ability to remove metal ions, the duration of the experiment varied from 15 minutes to 180 minutes. Figure 11, shows the percentage of Cd^{2+} and Pb^{2+} ions removed as a function of time.

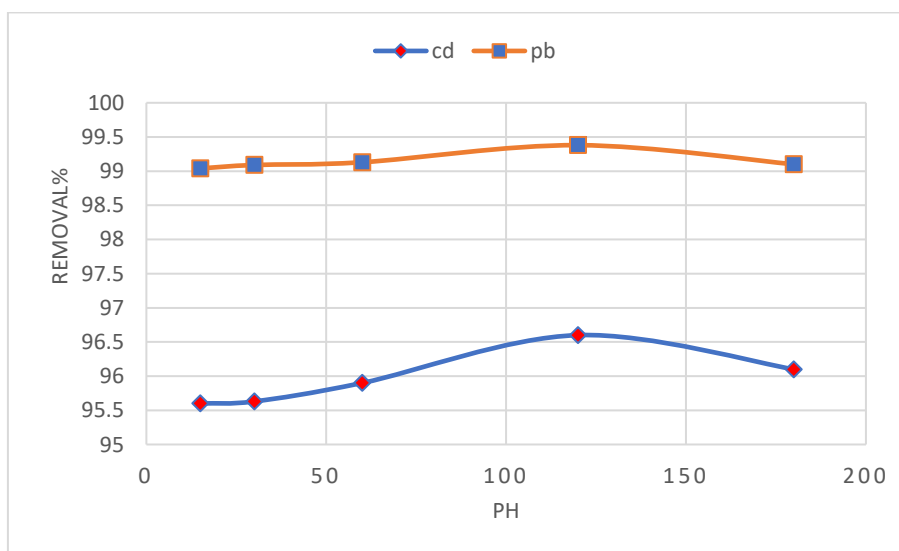


Fig.11. Effect of Time on adsorption of Cadmium ion, lead ion on (AM-CO-AN)/resole semi-IPNs

Study the Effect of Biological Efficacy:

After conducting the work method used in the dilution of IPNs and testing its effectiveness in inhibiting bacteria and

preventing their growth, it was found in the end that the IPNs used separately. He has the ability to inhibit the growth of bacteria at a different concentration level. Where this

appeared by preventing the growth or reproduction of bacteria used in this test and as follows.

The poly (Acrylamide-co Acrylonitrile)/resole-semi-IPNs, showed results with a high effect by inhibiting the growth of bacteria at a concentration level of 6, i.e. at the sixth tube (Wikler, M. A. (2006).

CONCLUSION

This study demonstrates that Cd (II), and Pb (II) may be effectively removed from aqueous solutions using (AM-co-AN)/resole semi-IPNs. Several conditions, such as contact time and initial pH, were tested to see how they affected the adsorption of these metals. The optimal pH of a solution for Cd (II) absorption. Pb (II) extracted from aqueous solution. The Langmuir monolayer sorption model was used to predict the sorption of Cadmium by AM-co-AN/resole semi-IPNs, whereas the Freundlich multilayer sorption model was utilized to predict the sorption of lead. IPNs, he has high effectiveness and effect in inhibiting *Streptococcus pyogenes* bacteria.

REFERENCES

- Allin, S. B. (2001). Introduction to Physical Polymer Science, (Sperling, LH).
- Anirudhan, T. S., Suchithra, P. S., & Divya, L. (2009). Adsorptive potential of 2-mercaptopbenzimidazole-immobilized organophilic hydrotalcite for mercury (II) ions from aqueous phase and its kinetic and equilibrium profiles. *Water, air, and soil pollution*, 196, 127-139.
- Carioscia, J. A., Stansbury, J. W., & Bowman, C. N. (2007). Evaluation and control of thiol-ene/thiol-epoxy hybrid networks. *Polymer*, 48(6), 1526-1532.
- Chen, S., Wang, Q., & Wang, T. (2011). Hydroxy-terminated liquid nitrile rubber modified castor oil-based polyurethane/epoxy IPN composites: Damping, thermal and mechanical properties. *Polymer Testing*, 30(7), 726-731.
- Chen, S., Wang, Q., Pei, X., & Wang, T. (2010). Dynamic mechanical properties of castor oil-based polyurethane/epoxy graft interpenetrating polymer network composites. *Journal of applied polymer science*, 118(2), 1144-1151.
- Crivello, J. V. (2007). Hybrid free radical/cationic frontal photopolymerizations. *Journal of Polymer Science Part A: Polymer Chemistry*, 45(18), 4331-4340.
- Decker, C., Bianchi, C., Decker, D., & Morel, F. (2001). Photoinitiated polymerization of vinyl ether-based systems. *Progress in Organic Coatings*, 42(3-4), 253-266.
- Dragan, E. S. (2014). Design and applications of interpenetrating polymer network hydrogels. A review. *Chemical Engineering Journal*, 243, 572-590.
- Inamdar, A., Cherukattu, J., Anand, A., & Kandasubramanian, B. (2018). Thermoplastic-toughened high-temperature cyanate esters and their application in advanced composites. *Industrial & Engineering Chemistry Research*, 57(13), 4479-4504.
- Jian, Y., He, Y., Sun, Y., Yang, H., Yang, W., & Nie, J. (2013). Thiol-epoxy/thiol-acrylate hybrid materials synthesized by photopolymerization. *Journal of Materials Chemistry C*, 1(29), 4481-4489.
- Lee, Y., Kim, D. N., Choi, D., Lee, W., Park, J., & Koh, W. G. (2008). Preparation of interpenetrating polymer network composed of poly (ethylene glycol) and poly (acrylamide) hydrogels as a support of enzyme immobilization. *Polymers for Advanced Technologies*, 19(7),

- 852-858.
- MA, W. (2006). Methods for dilution antimicrobial susceptibility tests for bacteria that grow aerobically: approved standard. *Clsi (Nccls)*, 26, M7-A7.
- Millar, J. R. (1960). 263. Interpenetrating polymer networks. Styrene–divinylbenzene copolymers with two and three interpenetrating networks, and their sulphonates. *Journal of the Chemical Society (Resumed)*, 1311-1317.
- Mokhtar, S. M., Elsabee, M. Z., Abd-Elaziz, S. M., & Gomaa, F. A. (2014). Synthesis, characterizations and polymerization of novel cyanoacrylamide derivative. *American Journal of Polymer Science*, 4(5), 123-129.
- Moussa, K., & Decker, C. (1993). Semi-interpenetrating polymer networks synthesis by photocrosslinking of acrylic monomers in a polymer matrix. *Journal of Polymer Science Part A: Polymer Chemistry*, 31(10), 2633-2642.
- Pfaller, M. A., Andes, D., Diekema, D. J., Espinel-Ingroff, A., Sheehan, D., & CLSI Subcommittee for Antifungal Susceptibility Testing. (2010). Wild-type MIC distributions, epidemiological cutoff values and species-specific clinical breakpoints for fluconazole and Candida: time for harmonization of CLSI and EUCAST broth microdilution methods. *Drug Resistance Updates*, 13(6), 180-195.
- Rajaraman, S. K., Mowers, W. A., & Crivello, J. V. (1999). Novel hybrid monomers bearing cycloaliphatic epoxy and 1-propenyl ether groups. *Macromolecules*, 32(1), 36-47.
- Ramya, R., Sankar, P., Anbalagan, S., & Sudha, P. N. (2011). Adsorption of Cu (II) and Ni (II) ions from metal solution using crosslinked chitosan-g-acrylonitrile copolymer. *International journal of environmental sciences*, 1(6), 1323-1338.
- Rudin, A., & Choi, P. (2012). *The elements of polymer science and engineering*. Academic press.
- Sangeetha, V., Kanagathara, N., Sumathi, R., Sivakumar, N., & Anbalagan, G. (2013). Spectral and thermal degradation of melamine cyanurate. *Journal of Materials Chemistry*, 2013, 262094.
- Sangermano, M., Cook, W. D., Papagna, S., & Grassini, S. (2012). Hybrid UV-cured organic–inorganic IPNs. *European polymer journal*, 48(10), 1796-1804.
- Sangermano, M., Razza, N., & Crivello, J. V. (2014). Cationic UV-curing: Technology and applications. *Macromolecular Materials and Engineering*, 299(7), 775-793.
- Xiao, P., Dumur, F., Graff, B., Gignes, D., Fouassier, J. P., & Lalevée, J. (2014). Blue Light Sensitive Dyes for Various Photopolymerization Reactions: Naphthalimide and Naphthalic Anhydride Derivatives. *Macromolecules*, 47(2), 601-608.
- Yang, J., Winnik, M. A., Ylitalo, D., & DeVoe, R. J. (1996). Polyurethane–Polyacrylate Interpenetrating Networks. 1. Preparation and Morphology. *Macromolecules*, 29(22), 7047-7054.